Photochemistry and Photobiology, Vol. 29, pp. 1163 to 1167
© Pergamon Press Ltd 1979. Printed in Great Britain
0031-8655/79/0601-1163$02.00/0

FÖRSTER TRANSFER RATES FOR CHLOROPHYLL *a**

LESTER L. SHIPMAN and DAVID L. HOUSMAN†
Chemistry Division, Argonne National Laboratory, Argonne, IL 60439, U.S.A.

(*Received* 13 *October* 1978; *accepted* 9 *February* 1979)

Abstract—A convenient formula has been derived for the calculation of Förster transfer rates between chlorophyll *a* molecules. The formula is applicable over limited ranges of absorption maxima positions, Stokes' shifts, solvents, relative orientations and intermolecular distances. The limitations on the applicability of the Förster transfer model are discussed. Finally, some implications for *in vivo* energy transfer are considered.

INTRODUCTION

The vast majority of chlorophyll (Chl) molecules *in vivo* function as antenna or light-gathering pigments which absorb photons and then transfer the resultant singlet excitation energy among each other until it is trapped by a few special Chl molecules in the photosynthetic reaction center. The excitation energy is then converted into useful chemical oxidizing and reducing capacity via a series of electron transfers. The mechanism of singlet excitation migration has long been the subject of study. For Chl whose excited singlet states are weakly coupled, the excitation is transferred via the Förster mechanism (Förster, 1948 and 1965). The subject of excitation transfer and some of its implications for photosynthesis have been covered in recent reviews by Knox (1975 and 1977).

We have noted that there is a significant need for a convenient formula for the calculation of Förster transfer rates between Chl *a* molecules, especially a formula that covers ranges of absorption maxima positions, Stokes' shifts, solvents, relative orientations and intermolecular distances. The derivation of such a formula is the subject of this paper.

FÖRSTER TRANSFER MECHANISM

The four state model of Förster transfer is described in Fig. 1 and Table 1. The system consists of molecules A and B and the surrounding solvent medium. The first symbol in parentheses following the letter designating the molecule (i.e. A or B) denotes the populated electronic state of the molecule and the second symbol denotes the electronic state for which the intramolecular geometry and solvent arrangement are appropriate. Thus, $A(S_1, S_0)$ means that molecule A is in its first excited electronic state, S_1, with an intramolecular geometry and solvent arrangement appropriate for its ground electronic state, S_0. All four states of the system are specified in Table 1. The Förster transfer rate constants are k_{AB} and k_{BA} (Fig. 1). The other two rate constants, designated 'fast relaxation' in Fig. 1, are the rate constants for thermal equilibration to a Boltzmann population of vibrational levels; this relaxation should be of the order 10^{12}–$10^{13}\ s^{-1}$ at 25°C.

FÖRSTER TRANSFER CYCLE

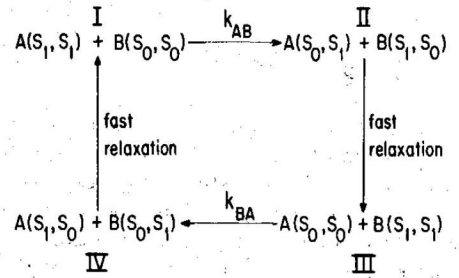

Figure 1. A four state diagram representing Förster transfer between molecules A and B. See text and Table 1 for a description of the symbols.

In the range of applicability of the Förster transfer mechanism, the equilibration rate constant is much faster than both k_{AB} and k_{BA}, and therefore the equilibrium populations of II and IV are quite small, while the ratio of the populations of I and III is k_{BA}/k_{AB}. An explicit form of the Förster transfer rate constant is given in the next section.

DERIVATION OF THE RATE FORMULA

A quantum mechanical derivation of the Förster transfer rate expression has been given by Förster (1965). Since we agree with Förster's derivation up to the point of departure for our derivation of an explicit formula for excitation transfer between chlorophyll *a*(Chl *a*) molecules, the derivation of Förster need not be repeated here. Our derivation

*This work was performed under the auspices of the Office of Basic Energy Sciences of the United States Department of Energy.

†A participant in the Undergraduate Research Participation Program administered by the Argonne Center for Education Affairs.

Table 1. Description of four state model for Förster transfer*

System state	Electronic State Mole. A	Mole. B	Population of vibrational levels	Electronic state for which the intramolecular geometry and solvent arrangement are appropriate Mole. A	Mole. B
I	S_1	S_0	Boltzmann	S_1	S_0
II	S_0	S_1	Non-Boltzmann	S_1	S_0
III	S_0	S_1	Boltzmann	S_0	S_1
IV	S_1	S_0	Non-Boltzmann	S_0	S_1

* See text and Fig. 1 for further explanation.

begins with Eq. 10.6 of Förster (1965). Specifically, the rate constant, k_{AB} (Fig. 1), is given by the following expression.*

$$k_{AB} = \frac{4\pi^2 10^{-24}}{h^2 c} \frac{[\mathbf{U}_A \cdot \mathbf{U}_B - 3(\mathbf{U}_A \cdot \mathbf{r}_{AB})(\mathbf{U}_B \cdot \mathbf{r}_{AB})]^2}{n^4 R_{AB}^6} \times \int_0^\infty \mu^2_{A,f}(\bar{\nu}) \cdot \mu^2_{B,a}(\bar{\nu})\, d\bar{\nu} \quad (1)$$

where $\mathbf{U}_A$ (unitless) and $\mathbf{U}_B$ (unitless) are unit vectors in the direction of the $S_0 \rightarrow S_1$ transition dipole on molecules A and B, respectively, $\mathbf{r}_{AB}$ (unitless) is a unit vector from the center of macrocycle A to the center of macrocycle B, R_{AB} (Å) is the distance from the center of macrocycle A to the center of macrocycle B, n (unitless) is the index of refraction of the solvent medium, h (erg-s) is Planck's constant, c (cm s^{-1}) is the speed of light in a vacuum, $\mu^2_{A,f}(\bar{\nu})$ (Debye^2 cm) is the $S_1 \rightarrow S_0$ dipole strength distribution for fluorescence from molecule A and $\mu^2_{B,a}(\bar{\nu})$ (Debye^2 cm) is the $S_0 \rightarrow S_1$ plus $S_0 \rightarrow S_2$ dipole strength distribution for light absorption by molecule B, and $\bar{\nu}$ (cm^{-1}) is the energy. The relationship between the dipole strength distribution and quantum mechanical transition dipole for Chl *a* has been previously discussed (Shipman, 1977a). The constants at the front of Eq. 1 have the following value.

$$\frac{4\pi^2 10^{-24}}{h^2 c} = 2.999 \times 10^{19}\,(\text{Å})^6\,\text{Debye}^{-4}\,\text{cm}^{-1}\,\text{s}^{-1}. \quad (2)$$

We turn now to the evaluation of the Förster overlap integral,

$$\left[\int_0^\infty\right] \mu^2_{A,f}(\bar{\nu})\mu^2_{B,a}(\bar{\nu})\, d\bar{\nu}. \quad (3)$$

From a deconvolution of the visible absorption spectrum of Chl *a* in diethyl ether (Shipman *et al.*, 1976) the following expression was derived (Shipman, 1977a) for the dipole strength distribution of the $S_0 \rightarrow S_1$ plus $S_0 \rightarrow S_2$ transitions,

$$\begin{aligned}\mu^2_{B,a}(\bar{\nu}) &= 3.03 \times 10^{-2} \exp\{-2.51 \times 10^{-5}[\bar{\nu} - (\bar{\nu}_B - 11)]^2\} \\ &+ 1.29 \times 10^{-2} \\ &\times \exp\{-7.81 \times 10^{-6}[\bar{\nu} - (\bar{\nu}_B + 89)]^2\} \\ &+ 6.07 \times 10^{-3} \\ &\times \exp\{-3.59 \times 10^{-6}[\bar{\nu} - (\bar{\nu}_B + 1149)]^2\} \\ &+ 2.93 \times 10^{-3} \\ &\times \exp\{-4.59 \times 10^{-6}[\bar{\nu} - (\bar{\nu}_B + 2299)]^2\}\end{aligned} \quad (4)$$

where $\bar{\nu}_B$ (cm^{-1}) is the position of the $S_0 \rightarrow S_1$ absorption maximum for molecule B. The first three terms in Eq. 4 have been assigned to $S_0 \rightarrow S_1$ and the fourth term in Eq. 4 has been assigned to a mixture of $S_0 \rightarrow S_1$ and $S_0 \rightarrow S_2$ (Shipman *et al.*, 1976). After making the assumption of mirror symmetry between the dipole strength distribution for absorption and the dipole strength distribution for fluorescence, the following expression is derived.

$$\begin{aligned}\mu^2_{A,f}(\bar{\nu}) &= 3.03 \times 10^{-2} \\ &\times \exp\{-2.51 \times 10^{-5}[\bar{\nu} - (\bar{\nu}_A + \Delta_A + 11)]^2\} \\ &+ 1.29 \times 10^{-2} \\ &\times \exp\{-7.81 \times 10^{-6}[\bar{\nu} - (\bar{\nu}_A + \Delta_A - 89)]^2\} \\ &+ 6.07 \times 10^{-3} \\ &\times \exp\{-3.59 \times 10^{-6}[\bar{\nu} - (\bar{\nu}_A + \Delta_A - 1149)]^2\} \\ &+ 2.93 \times 10^{-3} \\ &\times \exp\{-4.59 \times 10^{-6}[\bar{\nu} - (\bar{\nu}_A + \Delta_A - 2299)]^2\}\end{aligned} \quad (5)$$

where $\bar{\nu}_A$ (cm^{-1}) is the position of the $S_0 \rightarrow S_1$ absorption maximum of molecule A and Δ_A (cm^{-1}) is the energy of the $S_1 \rightarrow S_0$ fluorescence maximum minus the energy of the $S_0 \rightarrow S_1$ absorption maximum. Thus, Δ_A is the Stokes' shift for molecule A and is a *negative* quantity. The first three terms in Eq. 5 correspond to $S_1 \rightarrow S_0$ fluorescence and the fourth term is an overestimate of the $S_1 \rightarrow S_0$ contribution because it also contains a contribution from

*The factor of 10^{-24} which appears in our Eq. 1 and does not appear in Förster's Eq. 10.6 was introduced to convert units from Å to cm (R_{AB}) and from Debye^2 to esu^2 cm^2 (μ^2).

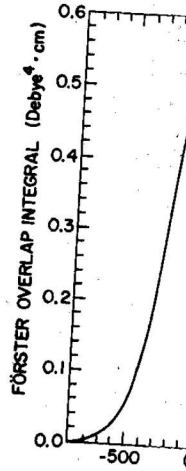

Figure 2. Förster ov
energy separation be
($\bar{\nu}_A + \Delta_A$) of molecule

$S_0 \rightarrow S_2$ which was
tion of mirror symm

When Eqs. 4 and
the integral is evalu
Förster overlap integr
is displayed as a das
when Eq. 4 and the
substituted into Eq.
lower bound to the
obtained; this result is
Fig. 2. Note that the
coalesce for $\bar{\nu}_A - \bar{\nu}_B +$
the product of two Ga
been used to obtain a
lower bound to the För

$$k_{AB} = 2.999 \times 10^{19} [\mathbf{U}_A$$

$$\times \{0.230 \exp[-1.26 \times$$
$$+ 0.242 \exp[-5.96 \times$$
$$+ 0.122 \exp[-3.14 \times$$
$$+ 0.0746 \exp[-3.90 \times$$
$$+ 0.0822 \exp[-2.46 \times$$
$$+ 0.0244 \exp[-1.80 \times$$
$$+ 0.0289 \exp[-3.88 \times$$
$$+ 0.0190 \exp[-2.89 \times$$
$$+ 0.0110 \exp[-2.01 \times$$

Because Eq. 6 was derived
the Förster overlap integra
at the end of Eq. 6 is the lo
the limits of applicability o

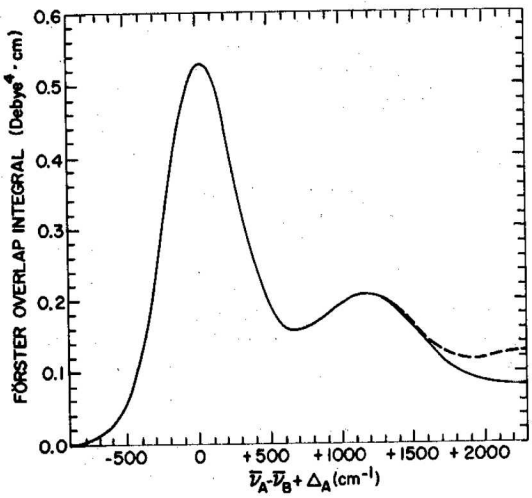

Figure 2. Förster overlap integral as a function of the energy separation between the fluorescence maximum ($\bar{\nu}_A + \Delta_A$) of molecule A and the absorption maximum ($\bar{\nu}_B$) of molecule B.

$S_0 \rightarrow S_2$ which was introduced through the assumption of mirror symmetry.

When Eqs. 4 and 5 are substituted into Eq. 3 and the integral is evaluated, an upper bound for the Förster overlap integral is obtained; this upper bound is displayed as a dashed curve in Fig. 2. Similarly, when Eq. 4 and the first three terms of Eq. 5 are substituted into Eq. 3 and the integral evaluated, a lower bound to the Förster overlap integral is obtained; this result is displayed as a solid curve in Fig. 2. Note that the upper and lower bound curves coalesce for $\bar{\nu}_A - \bar{\nu}_B + \Delta_A < 1200\,cm^{-1}$. The fact that the product of two Gaussians is itself a Gaussian has been used to obtain an analytic expression for the lower bound to the Förster transfer rate constant, k_{AB}.

$$k_{AB} = 2.999 \times 10^{19} \frac{[\mathbf{U}_A \cdot \mathbf{U}_B - 3(\mathbf{U}_A \cdot \mathbf{r}_{AB})(\mathbf{U}_B \cdot \mathbf{r}_{AB})]^2}{n^4 R_{AB}^6}$$

$$\times \{0.230 \exp[-1.26 \times 10^{-5}(\bar{\nu}_A - \bar{\nu}_B + \Delta_A + 22)^2]$$
$$+ 0.242 \exp[-5.96 \times 10^{-6}(\bar{\nu}_A - \bar{\nu}_B + \Delta_A - 78)^2]$$
$$+ 0.122 \exp[-3.14 \times 10^{-6}(\bar{\nu}_A - \bar{\nu}_B + \Delta_A - 1138)^2]$$
$$+ 0.0746 \exp[-3.90 \times 10^{-6}(\bar{\nu}_A - \bar{\nu}_B + \Delta_A - 178)^2]$$
$$+ 0.0822 \exp[-2.46 \times 10^{-6}(\bar{\nu}_A - \bar{\nu}_B + \Delta_A - 1238)^2]$$
$$+ 0.0244 \exp[-1.80 \times 10^{-6}(\bar{\nu}_A - \bar{\nu}_B + \Delta_A - 2298)^2]$$
$$+ 0.0289 \exp[-3.88 \times 10^{-6}(\bar{\nu}_A - \bar{\nu}_B + \Delta_A - 2288)^2]$$
$$+ 0.0190 \exp[-2.89 \times 10^{-6}(\bar{\nu}_A - \bar{\nu}_B + \Delta_A - 2388)^2]$$
$$+ 0.0110 \exp[-2.01 \times 10^{-6}(\bar{\nu}_A - \bar{\nu}_B + \Delta_A - 3448)^2]\}. \quad (6)$$

Because Eq. 6 was derived from the lower bound for the Förster overlap integral (*viz.*, the series expansion at the end of Eq. 6 is the lower bound curve of Fig. 2), the limits of applicability of Eq. 6 are $\bar{\nu}_A - \bar{\nu}_B + \Delta_A < 1200\,cm^{-1}$. The corresponding formula for k_{BA} is obtained by interchanging A and B in Eq. 6. The limits of applicability of the resulting formula are $\bar{\nu}_B - \bar{\nu}_A + \Delta_B < 1200\,cm^{-1}$.

LIMITATIONS

There are a number of limitations that should be considered before applying the Förster rate constant expression given in Eq. 6. Each of these limitations is discussed separately under subheadings as follows.

Temperature

Equation 6 was derived from a visible absorption spectrum recorded at 298 K and cannot be applied *accurately* for much lower temperatures, where the absorption and fluorescence peaks should be narrower, or for higher temperatures, where the peaks should be broader.

Coordination number

The Mg of Chl *a* is pentacoordinated in diethyl ether at 298 K. In more nucleophilic solvents such as pyridine, the Mg is hexacoordinated at 298 K and there is a significant change in the shape of the absorption spectrum (Shipman *et al.*, 1976). In less nucleophilic solvents such as diethyl ether, the Mg becomes hexacoordinated at low temperatures. Equation 6 applies *accurately* only for pentacoordinated Chl *a*.

Medium effects

In a previous study (Shipman, 1977a) the Lorentz model for the solvent medium was used to obtain a medium correction for the effect of solvent polarization on the effective electric field at the absorbing molecule. In addition, a dipole strength correction was made for the reduced speed of light in diethyl ether compared to vacuum (1/1.35 reduction) and the resultant increase in the radiation density. Thus, the starting point for the present analysis was a dipole strength distribution for absorption that was corrected, in an approximate way, to the dipole strength distribution expected for molecules in a medium of index of refraction 1 (i.e. vacuum). The n^{-4} factor in the rate expression (Eq. 6) is an attempt to account for the effect of the solvent medium in which molecules A and B reside. It is assumed that the transition dipole-transition dipole interaction energy will be reduced by the reciprocal of the high frequency dielectric constant (i.e. n^{-2}) of the solvent medium compared to the interaction energy in a vacuum. Since the interaction energy is squared in the rate expression, a factor of n^{-4} follows. As A and B approach each other to the point of close contact, the n^{-4} factor is a poorer approximation to the true effect of the solvent medium.

Transition densities

The Förster transfer rate is directly proportional to the square of the interaction energy between the

transition densities on molecules A and B. For intermolecular spacings large compared to the extent of the transition density on a molecule, the dipole–dipole term in a multipole expansion dominates the interaction energy. It is the dipole–dipole approximation to the interaction energy that appears in Eq. 6. Chang (1977) has explicitly considered the limits of applicability of the dipole–dipole approximation.

Character of the states

As implied in Fig. 1, it has been assumed that the electronic excitation is localized completely on one molecule or the other. For sufficiently strong transition density coupling, the electronic excitation will be delocalized with excitation extending over more than one molecule on a vibrational timescale. Since the transition density interaction falls off as R^{-3}, this is a more serious problem when the molecules are close together than when they are far apart. At close contact between Chl *a* molecules such that there is a significant overlap between the molecular orbitals on the interacting macrocycles, the charge transfer states corresponding to the transfer of an electron from A to B or vice versa can mix with the locally excited states and change the character of the excited states involved. Equation 6 does not take charge transfer states into account. Since the molecular orbital overlap falls off exponentially with separation between the macrocycles, the mixing in of charge transfer character is only important for short distances between the Chl *a* macrocycles.

Relaxation rate

In Fig. 1 and in Förster's derivation of the rate expression, the vibrational relaxation rate is assumed to be much faster than the Förster transfer rate. This vibrational relaxation rate can be estimated to lie in the 10^{12}–$10^{13}\,s^{-1}$ range. Thus, the rate expression of Eq. 6 is not accurate for Förster transfer rates approaching $10^{12}\,s^{-1}$. Again, this is a more serious problem when the molecules are brought close together because the Förster transfer rate falls off as R^{-6}.

A limit may be derived for the shortest distance between the centers of the Chl *a* macrocycles for which Eq. 6 is a good approximation. We require that the Förster transfer rate be much less than $10^{12}\,s^{-1}$ to meet the limit imposed by the vibrational relaxation rate. Taking the maximum Förster overlap integral (i.e. 0.53 D^4 cm), the maximum n^{-4} for solvents generally used in Chl studies ($1/1.3^4$), and the maximum orientational factor (i.e. 4), we find that the Förster transfer rate constant is always less than $10^{11}\,s^{-1}$ for $R_{AB} > 25$ Å. Also, at 25 Å the absolute value of the transition dipole–transition dipole interaction energy is less than $10\,cm^{-1}$, which is much smaller than the intramolecular vibrational transitions of Chl *a*. For such a small interaction energy, the relaxed states (I and III of Fig. 1) should not be significantly delocalized over more than one Chl *a* molecule. For $R_{AB} > 25$ Å, the edges of the Chl *a* macrocycle π-systems are separated by more than 13 Å; the intermolecular molecular orbital overlap between the π-systems should be so small that charge transfer character is not important to the description of the electronic states involved. Finally, the work of Chang (1977) indicates that the dipole–dipole term of the multipole expansion becomes a good approximation to the transition density–transition density interaction energy at $R_{AB} > 25$ Å. We conclude, for all of the above reasons, that Eq. 6 is a good representation of the singlet excitation transfer rate constant if the centers of the Chl *a* macrocycles are separated by at least 25 Å.

IMPLICATIONS FOR *IN VIVO* ENERGY TRANSFER

Because the average Chl concentration in the thylakoid membranes of green plants is $\sim 0.1\,M$, many Chl molecules may have neighboring Chl molecules closer than our 25 Å limit for the validity of Eq. 6. Nevertheless, it is worthwhile to consider the effect of the Franck–Condon factors (Förster overlap integral) on the rate of energy transfer *in vivo* using Eq. 6 as a first approximation to the true transfer rate constant.

As shown by Seely (1973) energy transfer from antenna Chls to photoreaction center Chls can be accelerated by optimal, non-random arrangement of Chl 'forms' such that the more red-shifted 'forms' are nearer and the less red-shifted 'forms' are farther away. The Förster overlap integral curve in Fig. 2 allows us to quantify this concept further. The maximal k_{AB} is obtained when the fluorescence maximum for molecule A is blue-shifted (i.e. at a higher energy) by $25\,cm^{-1}$ relative to the absorption maximum of molecule B. The four major 'forms' of Chl *a* *in vivo* have absorption maxima at $\sim$662, $\sim$670, $\sim$677 and $\sim$683 nm (Shipman, 1977b). Thus, the energy gap between sequential 'forms' is 130–181 cm^{-1}. For Chl *a* Stokes' shifts in the range of 105–156 cm^{-1}, a maximum Förster overlap integral between sequential 'forms' is obtained.

Now consider the implications of the Förster overlap curve in Fig. 2 for other than the maximum overlap. Figure 2 clearly shows that the k_{AB} rate constant falls off rapidly when the absorption maximum of molecule B is blue shifted relative to the fluorescence maximum of molecule A. The Förster overlap integral goes through a secondary maximum at $\bar{\nu}_A - \bar{\nu}_B + \Delta_A = 1172\,cm^{-1}$. This maximum has an interesting implication for the green plant antenna system because it means that there is a substantial Förster overlap integral, and therefore the possibility (given suitable R_{AB} and transition dipole orientations, Eq. 6) of a substantial transfer rate, from the blue-most Chl *b* 'form' (640 nm absorption maximum *in vivo*, estimated 648 nm fluorescence maximum) to the photoreaction

center P700 species. Thus, the two maxima in the Förster overlap integral in Fig. 2 span the green plant antenna system from Chl *b* at its higher energy end to P700 at its lower energy end.

REFERENCES

Förster, Th. (1948) *Ann. Physik* **2**, 55–75.

Förster, Th (1965) In *Modern Quantum Chemistry* (Edited by O. Sinanoğlu), pp. 93–137. Academic Press, New York.

Chang, J. C. (1977) *J. Chem. Phys.* **67**, 3901–3909.

Knox, R. S. (1975) In *Bioenergetics of Photosynthesis* (Edited by Govindjee), pp. 183–221. Academic Press, New York.

Knox, R. S. (1977) In *Primary Processes of Photosynthesis* (Edited by J. Barber), pp. 55–97. Elsevier, New York.

Seely, G. R. (1973) *J. Theor. Biol.* **40**, 189–199.

Shipman, L. L. (1977a) *Photochem. Photobiol.* **26**, 287–292.

Shipman, L. L. (1977b) *J. Phys. Chem.* **81**, 2180–2184.

Shipman, L. L., T. M. Cotton, J. R. Norris and J. J. Katz (1976) *J. Am. Chem. Soc.* **98**, 8222–8230.